SLAC-PUB-884
March 1971

A STUDY OF THE REACTION $\pi^- p \to \rho^0 n$ AT 15 GeV/c *

F. Bulos, R. K. Carnegie, G. E. Fischer, E. E. Kluge,
D.W.G.S. Leith, H. L. Lynch, B. Ratcliff, B. Richter,
H. H. Williams, and S. H. Williams

Stanford Linear Accelerator Center
Stanford University, Stanford, California 94305

and

M. Beniston

IBM, Palo Alto, California 94304

ABSTRACT

The results of a wire spark chamber experiment studying the reaction $\pi^- p \to \pi^+ \pi^- n$ at 15 GeV/c are presented. The differential cross section, π-π mass distribution and density matrix elements have been determined from 10,000 $\pi\pi n$ events ($M_{\pi\pi} < 1.0$ GeV) produced with $-t < .30$ $(\text{GeV/c})^2$. Both the density matrix elements and the differential cross section exhibit structure in the forward direction ($-t < m_\pi^2$).

(A shorter version of this paper was submitted to Phys. Rev. Letters.)

* Work supported by the U. S. Atomic Energy Commission.

We report the results of a wire spark chamber experiment performed at SLAC to study the reaction $\pi^- p \to \pi^+ \pi^- n$ at an incident beam momentum of 15 GeV/c.[1] This reaction has been previously studied at lower energies,[2] but prior to this experiment no accurate determination of the density matrix elements or the differential cross section, $d\sigma/dt$, has been available at high energies ($t \equiv$ momentum transfer squared to the nucleon). In addition, knowledge of these quantities for very small momentum transfers has been lacking at all energies. Absorption models[3] and also the vector dominance model (VDM) predict that the $\pi^- p \to \rho^0 n$ differential cross section for transversely polarized rho mesons should have a sharp rise in the forward direction, ($-t < m_\pi^2$), as does the reaction $\gamma N \to \pi^\pm N$. For a detailed comparison of the data with VDM, see Ref. 4.

The experimental apparatus, which is described in more detail elsewhere,[5] is shown in Fig. 1. The momentum of the incident π^- was determined to an accuracy of $\pm .3\%$ and the horizontal and vertical projected π^- angles at the target were determined to an accuracy of $\pm .5$ mr by counter hodoscopes placed in the beam line. The spectrometer, which measured the momenta and angles of the outgoing pions, consisted of seven 2-gap spark chambers, an analyzing magnet ($100 \times 38 \times 120$ cm aperture), and trigger hodoscopes. Three chambers were placed upstream of the magnet and four downstream. The inside faces of the magnet gap were lined with scintillation counters to veto events in which a particle intersected the pole faces. The trigger logic required an incident beam particle, two or more charged particles downstream of the magnet, and no signal from the magnet veto counters. In addition, scintillator-Pb sandwich counters surrounded the 1 m long LH_2 target to detect particles which escaped the spectrometer. A gas Čerenkov counter placed downstream of the spectrometer distinguished π's from heavier particles. The information from both the Čerenkov counter and target counters was used only in the off-line analysis.

Because the main pion beam passed through the spectrometer system, and because of the high instantaneous fluxes ($8\,\pi^-/1.6\,\mu$sec burst), a small region of the chambers was desensitized by the installation of a polyurethane plug. As a result, very asymmetric ρ decays could not be observed. This limitation of the plug was matched by the low momentum cutoff of the magnet which also prohibited observation of very asymmetric decays. For $|\cos\theta| < .8$ (where θ is the polar angle of the π^- in the helicity frame), the average acceptance was 25%, and varied slowly as a function of $M_{\pi\pi}$ and t for ρ-n events. The π-π mass resolution was less than ±10 MeV at the mass of the rho; the missing mass resolution was ±80 MeV, and the t resolution was calculated to be $\pm 0.016\ \sqrt{-t}\ (\mathrm{GeV/c})^2$.

The density matrix elements of the di-pion system were determined as a function of t by fitting the observed decay angular distribution to the form $\omega(\theta,\phi) = W(\theta,\phi)\ E(\theta,\phi)$ where

$$W(\theta,\phi) = \frac{1}{4\pi}\Big[1 + (\rho_{00}-\rho_{11})(3\cos^2\theta - 1) + 2\sqrt{3}\,\mathrm{Re}(\rho_{0S})\cos\theta - 3\sqrt{2}\,\mathrm{Re}(\rho_{10})\sin 2\theta\cos\phi - 2\sqrt{6}\,\mathrm{Re}(\rho_{1S})\sin\theta\cos\phi - 3\rho_{1-1}\sin^2\theta\cos 2\phi\Big] \qquad (1)$$

is the angular distribution for S and P waves, $E(\theta,\phi)$ is the detection efficiency of the spectrometer, and θ,ϕ are the polar and azimuthal decay angles of the π^- in the ρ rest frame. The normalization of the density matrix elements was $\rho_{00}+2\rho_{11}+\rho_{00}^S=1$. The analysis was performed on the events in the mass interval $.665 < M_{\pi\pi} < .865$ GeV. A Monte Carlo program was used to calculate $E(\theta,\phi)$ to correct for geometrical losses. By refitting the data with more restrictive geometrical cutoffs than those imposed by the apparatus, it was ascertained that the ρ_{ij} obtained were not affected by the geometry of the apparatus. The density matrix elements were obtained in the helicity (ρ_{ij}^H) and Jackson (ρ_{ij}^J) frames

and their consistency checked by rotating from one frame to the other. By varying the missing mass cutoff and using the information from the target counters, it was determined that 12 ± 2% of the event sample was $\pi^+\pi^-N^*$ events and that this contribution did not affect the values of ρ_{ij}.[6]

Recently Biswas et al.[7] have suggested that higher partial waves than ℓ=1 may contribute in the ρ region of $\pi\pi$ mass. They find that their 4 GeV data are inconsistent with the relation $\langle \cos 2\phi \rangle = -\frac{3}{4}\rho_{1-1}\sin^2\theta$ which is valid if only S and P waves are present, and they also find ρ_{1-1} to be mass dependent. Our data show no evidence of these discrepancies: $\langle \cos 2\phi \rangle$ is consistent with $-\frac{3}{4}\rho_{1-1}\sin^2\theta$ ($\chi^2 = 16.5$ for 18 degrees of freedom) and there is no evidence for a mass dependence of ρ_{1-1} ($\chi^2 = 10.6$ for 10 degrees of freedom).[8] In addition, there are no systematic deviations of the fit from the data in any particular region of $\cos\theta, \phi$. Hence, we conclude that partial waves with $\ell \geq 2$ are not required to describe the decay angular distribution.

The density matrix elements are shown in Figs. 2a-e and 3a-e, and are listed in Tables 1 and 2. The error bars shown are statistical only; systematic errors, which could result if there were small unknown biases in the apparatus or event reconstruction, are estimated to be less than the statistical errors. The fact that Re ρ_{0S} and Re ρ_{1S} do not vanish is conclusive evidence that the dipion system may not be described by a pure P wave.

Many of the density matrix elements exhibit structure for momentum transfers less than m_π^2; in particular there is a striking dip in $\rho_{00}-\rho_{11}$ (helicity and Jackson frames) and in Re ρ^J_{10} for $-t < m_\pi^2/2$, a region which has not been studied in previous experiments.[9] The narrow dip in $\rho_{00}-\rho_{11}$ is predicted by one-pion-exchange absorption models (OPEA).[3] OPEA also predicts that $\rho^J_{1-1} \approx 0$ for $-t < m_\pi^2$, as is observed in the data.

It is not possible to determine separately ρ_{11} or ρ_{00}^S from the angular distribution alone; however, the Schwartz inequalities on the helicity amplitudes and the requirement that the diagonal elements of the density matrix be positive-definite enable one to establish limits on ρ_{00}^S and ρ_{11}. The limits on ρ_{11} calculated in this manner are shown in Figs. 2f and 3f.

Independent information on ρ_{00}^S (and hence ρ_{11}) may be obtained from the existing $\pi^- p \to \pi^o \pi^o n$ data.[10] The curves in Figs. 2f and 3f show the values of ρ_{11} calculated assuming $d\sigma/dt\,(\text{S-wave}) \propto |t| e^{7t}/(t-m_\pi^2)^2$, which is a good representation of the t-dependence of the $\pi^o\pi^o$ data; the normalization was obtained by scaling the $\pi^o\pi^o$ cross section to 15 GeV.[11] The values of ρ_{11} obtained in this manner are consistent with the limits described above. We have also calculated ρ_{11} taking the amount of S-wave from our fits to the π-π mass spectrum (see discussion below) and assuming the same t-dependence as above. The results obtained agree within errors.

A peak in the calculated value of ρ_{11} is observed in the forward direction. The structure does not strongly depend on the details of the S-wave t-dependence; for example, if the S-wave is assumed to decrease by only 25% from $t=-m_\pi^2$ to $t=t_{min}$, rather than vanishing as predicted by OPEA, the peak in ρ_{11} is decreased by only 20%.

The total differential cross section $d\sigma/dt\ (\pi^- p \to \pi^+ \pi^- n)$ and the transversely polarized cross section in the helicity frame, $2\rho_{11}^H \frac{d\sigma}{dt}(\pi^- p \to \pi^+ \pi^- n)$, are shown in Fig. 4 for the mass interval $.665 < M_{\pi\pi} < .865$ GeV. The transverse and longitudinal cross sections for the Jackson frame are shown in Fig. 5. The cross sections are listed in Table 3. The error in the overall normalization is $\pm 5\%$ and results from uncertainties in the counter and spark chamber efficiencies, thick target corrections, and track reconstruction efficiency. As a check on our

absolute normalization, we have measured the elastic cross section, $\frac{d\sigma}{dt}(\pi^- p \to \pi^- p)$, with the same apparatus. Our measurements agree well with those of Foley et al.[12] as shown in Fig. 6.

The sharp rise in the helicity transverse cross section and the dip in the total cross section are predicted by OPEA models and verify that the reaction is dominated by pion exchange for small momentum transfers. The transverse cross section in the Jackson frame is expected to be flat (i.e., no peak or dip); this is consistent with the data. The total rho cross section, which is also shown in Fig. 4, has been obtained from the $\pi^+\pi^-$ cross section by subtracting the amount of S-wave and correcting for the fraction of the rho mass spectrum outside our mass interval. The normalization error is ±25%, the dominant contribution coming from the uncertainty in the rho line shape.

The π-π mass distribution shown in Fig. 7 is described from .4 - .9 GeV using only a P-wave resonance and an S-wave background. The P-wave is parameterized by a Breit-Wigner form which was used by Pišut and Roos[13] to fit both ρ^- and ρ^0 mass distributions at lower energies:

$$\frac{d\sigma}{dm} \propto \frac{1}{q} \frac{m^2 m_0^2 \Gamma_\ell^2(m)}{\left(m_0^2 - m^2\right)^2 + m_0^2 \Gamma_\ell^2(m)} \int_{t_{min}(m)}^{T} e^{At} dt$$

where $\Gamma_\ell(m) = \Gamma_0 \left(\frac{q}{q_0}\right)^{2\ell+1} \frac{m_0}{m} \frac{1+R^2 q_0^2}{1+R^2 q^2}$; ℓ = angular momentum of resonance,

$$q = \left(\frac{m^2}{4} - m_\pi^2\right)^{1/2}$$

$$q_0 = \left(\frac{m_0^2}{4} - m_\pi^2\right)^{1/2}$$

m_0, Γ_0 = the mass and width,

A is the slope of $d\sigma/dt(\pi^- p \to \rho^0 n)$,

$t_{min}(m)$ is the kinematical lower limit of t,

T is the upper limit of |t| for the event sample, and

R is a parameter which corresponds to the range of the interaction.

The S-wave contribution is also parameterized by the above form with a mass of .7 GeV and a width of .4 GeV; this is consistent with the $\pi^o\pi^o$ mass distribution.[10] The fit yields a rho mass and width of $M_\rho = .771 \pm .004$ GeV, $\Gamma_\rho = .160 \pm .014$ GeV, and $R^2 = 4.8 \pm 3.2$ $(GeV/c)^{-2}$. The amount of S-wave required is $11 \pm 2\%$ which agrees well with the 12% predicted by scaling the $\pi^o\pi^o n$ data.[11] Other acceptable fits to the mass spectrum may also be obtained by changing R or by choosing different Breit-Wigner functions, such as the standard P-wave form discussed by Jackson.[14] Although these forms are indistinguishable within the interval .4 - .9 GeV, the high mass behavior results in normalizations differing by $\pm 20\%$. Since this region is complicated by the presence of other resonances, it is difficult to distinguish between the forms by extending the fits to higher masses.

We summarize our results as follows: The dipion density matrix elements have been determined as a function of t for $.665 < M_{\pi\pi} < .865$ GeV and exhibit pronounced structure at small momentum transfers. We note that the angular distribution is well described by S and P waves alone. The differential cross sections for $\pi^- p \rightarrow \rho^o n$ and $\pi^- p \rightarrow \pi^+\pi^- n$ for the above mass interval have also been determined. The total and longitudinal cross sections show a dip at small t, whereas the transverse cross section in the helicity frame has a strong forward peak.

FOOTNOTES AND REFERENCES

1. These results supersede the preliminary data presented at the XVth International Conference on High Energy Physics, Kiev (1970).
2. B. D. Hyams et al., Nucl. Phys. B7, 1 (1968); P. B. Johnson et al., Phys. Rev. 176, 1651 (1968); J. P. Baton and G. Laurens, Phys. Rev. 176, 1574 (1968). Additional references may be found in these papers.
3. K. Gottfried and J. D. Jackson, Nuovo Cimento 34, 735 (1964); F. Henyey, G. L. Kane, Jon Pumplin, and M. H. Ross, Phys. Rev. 182, 1579 (1969).
4. F. Bulos et al., "A comparison of $\pi^- p \to \rho^0 n$ with single pion photoproduction," Report No. SLAC-PUB-885, submitted to Phys. Rev. Letters. This article contains a list of references on VDM.
5. G. T. Armstrong et al., "Wire chamber spectrometer at SLAC," Report No. SLAC-PUB-801 (1970).
6. This event sample was selected by making both missing mass and target-counter cuts. The missing mass cut was .8 - 1.06 GeV; the cut on the targer-counter information was such that ≈30% of the $\pi^+\pi^- N^*$ events were removed while the $\pi^+\pi^- n$ events were unaffected.
7. N. N. Biswas et al., Phys. Rev. D1, 2705 (1970).
8. These checks were made on the data sample $-.1 < t < 0$ $(GeV/c)^2$ and $.665 < M_{\pi\pi} < .865$ GeV.
9. The region $-t < m_\pi^2/2$ is inaccessible to low energy experiments because of kinematical limits on t. For example, t_{min} (4 GeV) $\approx m_\pi^2/3$ whereas t_{min} (15 GeV) $\approx m_\pi^2/50$.
10. P. Sonderegger and P. Bonamy, Lund International Conference on Elementary Particles (Abstract 372) (1969); E. I. Shibata, D. H. Frisch, and M. A. Wahlig, Phys. Rev. 25, 1227 (1970).

11. The $\pi^o\pi^o$n data were scaled according to p^{-2} where p is the incident beam energy. Sonderegger and Bonamy (Ref. 10) have shown that this scaling works well over a range of 3 to 18 GeV/c. It has been assumed that the $\pi^o\pi^o$ cross section is I=0.

12. K. J. Foley et al., Phys. Rev. 181, 1775 (1969).

13. J. Pišut and M. Roos, Nucl. Phys. B6, 325 (1968).

14. J. D. Jackson, Nuovo Cimento 34, 1644 (1964).

FIGURE CAPTIONS

1. A plan view of the experimental apparatus.

2. (a-e) The density matrix elements in the helicity frame for $.665 < M_{\pi\pi} < .865$ GeV. The error bars indicate the statistical errors. (f) The upper and lower limits on ρ_{11} which are determined from the Schwartz inequalities on the helicity amplitudes and the requirement that the diagonal density matrix elements be positive definite. The errors on the limits result from the propagation of the errors on the density matrix elements. The curve is the calculated value of ρ_{11}^{H} obtained when the amount of S-wave is estimated from the $\pi^- p \to \pi^o \pi^o n$ data.

3. The density matrix elements evaluated in the Gottfried-Jackson frame. See the discussion in the caption of Fig. 2.

4. The total and transverse differential cross sections (helicity frame) as a function of momentum transfer for $\pi^- p \to \pi^+ \pi^- n$, $.665 < M_{\pi\pi} < .865$ GeV and the total cross section for $\pi^- p \to \rho^o n$. The error bars indicate the statistical errors.

5. The longitudinal and transverse differential cross sections in the Jackson frame for $\pi^- p \to \pi^+ \pi^- n$, $.665 < M_{\pi\pi} < .865$ GeV.

6. A comparison of $d\sigma/dt$ ($\pi^- p \to \pi^- p$) as measured in this experiment with the measurements of Foley et al.[12]

7. The observed $\pi^+ \pi^-$ mass spectrum for $|t| < 0.02$ $(GeV/c)^2$. The curve represents the fit described in the text, after it has been folded with the acceptance.

TABLE 1

Density Matrix Elements Evaluated in the Helicity Frame for $\pi^- p \to \pi^+ \pi^- n$, $.665 < M_{\pi\pi} < .865$ GeV

$-t$ (GeV/c)^2	$\rho^H_{00}-\rho^H_{11}$	Re ρ^H_{10}	ρ^H_{1-1}	Re ρ^H_{0S}	Re ρ^H_{1S}	$\rho^{H\ *}_{11}$
t_{min} - .0025	.248 ± .127	-.067 ± .040	-.025 ± .033	.296 ± .048	-.038 ± .021	.228 ± .042
.0025 - .0050	.595 ± .080	-.053 ± .031	.023 ± .020	.180 ± .045	-.048 ± .012	.097 ± .027
.0050 - .0075	.699 ± .061	-.034 ± .030	.015 ± .020	.202 ± .042	-.022 ± .011	.054 ± .020
.0075 - .0100	.734 ± .054	-.079 ± .028	.014 ± .016	.257 ± .037	-.029 ± .010	.038 ± .018
.0100 - .0125	.778 ± .045	-.068 ± .035	.015 ± .016	.268 ± .038	-.010 ± .009	.024 ± .015
.0125 - .0200	.722 ± .033	-.020 ± .010	.044 ± .010	.280 ± .020	.005 ± .006	.038 ± .011
.0200 - .0275	.760 ± .028	.028 ± .013	.038 ± .010	.280 ± .020	.017 ± .005	.031 ± .009
.0275 - .0350	.734 ± .036	.037 ± .015	.039 ± .011	.283 ± .023	.012 ± .007	.034 ± .012
.035 - .045	.705 ± .035	.078 ± .016	.040 ± .012	.247 ± .023	.022 ± .007	.040 ± .012
.045 - .060	.644 ± .034	.098 ± .014	.035 ± .012	.274 ± .021	.037 ± .007	.057 ± .011
.060 - .080	.656 ± .033	.145 ± .013	.023 ± .011	.240 ± .020	.045 ± .006	.061 ± .011
.080 - .100	.580 ± .047	.174 ± .017	.017 ± .018	.219 ± .026	.057 ± .009	.079 ± .016
.100 - .150	.454 ± .039	.186 ± .012	.019 ± .016	.225 ± .020	.077 ± .008	.123 ± .013
.150 - .200	.250 ± .073	.203 ± .020	.024 ± .027	.194 ± .012	.077 ± .012	.197 ± .024
.200 - .300	-.086 ± .099	.211 ± .022	.041 ± .034	.077 ± .033	.053 ± .016	.306 ± .033

*Note: The values of ρ^H_{11} are not directly measured and depend on certain assumptions concerning the S-wave. See discussion in text.

TABLE 2

Density Matrix Elements Evaluated in the Jackson Frame for $\pi^- p \to \pi^+ \pi^- n$, $.665 < M_{\pi\pi} < .865$ GeV

$-t$ (GeV/c)^2	$\rho^J_{00}-\rho^J_{11}$	Re ρ^J_{10}	ρ^J_{1-1}	Re ρ^J_{0S}	Re ρ^J_{1S}	ρ^J_{11} *
t_{min} - .0025	.206 ± .128	-.076 ± .040	-.033 ± .034	.306 ± .047	-.055 ± .021	.243 ± .043
.0025 - .005	.482 ± .090	-.117 ± .031	.002 ± .022	.173 ± .046	-.074 ± .015	.136 ± .030
.005 - .0075	.586 ± .068	-.141 ± .029	-.007 ± .021	.203 ± .042	-.057 ± .013	.092 ± .023
.0075 - .010	.579 ± .055	-.187 ± .027	-.030 ± .019	.254 ± .035	-.072 ± .010	.090 ± .018
.010 - .0125	.584 ± .063	-.216 ± .030	-.049 ± .021	.258 ± .038	-.069 ± .009	.089 ± .021
.0125 - .020	.557 ± .037	-.181 ± .009	-.007 ± .012	.267 ± .020	-.063 ± .008	.094 ± .012
.020 - .0275	.590 ± .033	-.185 ± .011	-.012 ± .011	.260 ± .020	-.062 ± .008	.088 ± .011
.0275 - .035	.541 ± .043	-.200 ± .005	-.021 ± .013	.274 ± .021	-.085 ± .008	.098 ± .014
.035 - .045	.559 ± .038	-.195 ± .012	-.005 ± .013	.235 ± .021	-.071 ± .009	.089 ± .013
.045 - .060	.479 ± .040	-.183 ± .011	-.005 ± .015	.257 ± .020	-.079 ± .009	.113 ± .013
.060 - .080	.525 ± .036	-.205 ± .011	-.011 ± .014	.229 ± .019	-.076 ± .008	.104 ± .012
.080 - .100	.492 ± .038	-.213 ± .015	-.004 ± .017	.216 ± .024	-.071 ± .009	.108 ± .013
.100 - .150	.374 ± .039	-.189 ± .009	.027 ± .019	.225 ± .020	-.072 ± .009	.150 ± .013
.150 - .200	.252 ± .062	-.172 ± .023	.064 ± .037	.182 ± .026	-.083 ± .015	.196 ± .021
.200 - .300	.185 ± .071	-.134 ± .023	.168 ± .042	.106 ± .029	-.036 ± .019	.216 ± .024

*Note: The values ρ^J_{11} are not directly measured and are dependent on certain assumptions concerning the S-wave. See discussion in text.

TABLE 3

Differential Cross Sections for $\pi^- p \to \pi^+ \pi^- n$

$-t$ $(GeV/c)^2$	$\frac{d\sigma}{dt}(\pi\pi)$ $\mu b/(GeV/c)^2$	$\rho_{11}^H \frac{d\sigma}{dt}(\pi\pi)$ * $\mu b/(GeV/c)^2$	$\rho_{11}^J \frac{d\sigma}{dt}(\pi\pi)$ * $\mu b/(GeV/c)^2$	$\frac{d\sigma}{dt}(\rho)$ * $\mu b/(GeV/c)^2$
t_{min} - .0025	221 ± 29	50.5 ± 11.4	53.6 ± 11.7	368 ± 51
.0025 - .005	307 ± 36	29.9 ± 8.9	41.6 ± 10.4	487 ± 65
.005 - .0075	332 ± 36	17.9 ± 7.0	30.6 ± 8.2	511 ± 65
.0075 - .010	344 ± 36	13.0 ± 6.3	30.8 ± 7.0	521 ± 64
.010 - .0125	377 ± 38	9.2 ± 5.8	33.7 ± 8.6	574 ± 68
.0125 - .020	355 ± 17	13.6 ± 4.0	33.2 ± 4.7	531 ± 30
.020 - .0275	375 ± 23	11.7 ± 3.5	33.1 ± 4.6	572 ± 41
.0275 - .035	301 ± 21	10.1 ± 3.7	29.4 ± 4.8	448 ± 38
.035 - .045	250 ± 17	10.0 ± 3.0	22.3 ± 3.5	368 ± 30
.045 - .060	195 ± 12	11.2 ± 2.3	21.9 ± 3.0	284 ± 22
.060 - .080	168 ± 10	10.2 ± 1.9	17.5 ± 2.3	252 ± 18
.080 - .100	111 ± 8.5	8.7 ± 1.8	12.0 ± 1.7	162 ± 15
.100 - .150	74.1 ± 3.9	9.1 ± 1.1	11.1 ± 1.1	109 ± 7.0
.150 - .200	44.7 ± 3.5	8.8 ± 1.3	8.8 ± 1.2	67.0 ± 6.3
.200 - .300	20.5 ± 1.7	6.3 ± 0.8	4.4 ± 0.6	30.5 ± 3.0

$$\frac{d\sigma}{dt}(\pi\pi) \equiv \frac{d\sigma}{dt}(\pi^- p \to \pi^+ \pi^- n), \quad .665 < M_{\pi\pi} < .865 \text{ GeV}$$

$$\frac{d\sigma}{dt}(\rho) \equiv \frac{d\sigma}{dt}(\pi^- p \to \rho^o n)$$

*Note: The values of $\rho_{11}^H \frac{d\sigma}{dt}$, $\rho_{11}^J \frac{d\sigma}{dt}$, and $\frac{d\sigma}{dt}(\rho)$ are not directly measured and depend on certain assumptions concerning the S-wave. See discussion in text.

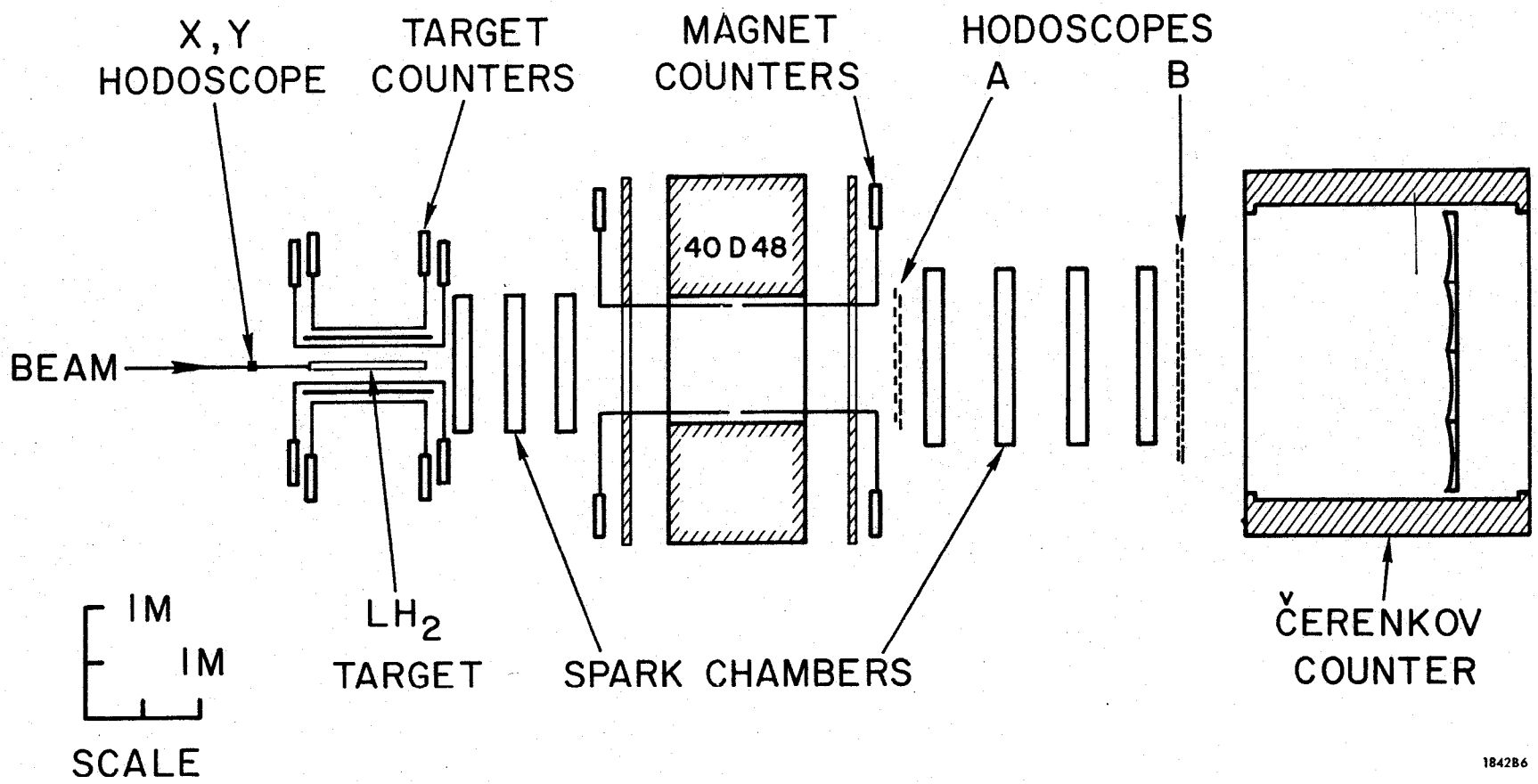
X, Y
HODOSCOPE
TARGET
COUNTERS
MAGNET
COUNTERS
HODOSCOPES
A
B
40 D 48
BEAM
IM
IM
SCALE
LH2
TARGET
SPARK CHAMBERS
ČERENKOV
COUNTER
1842B6

Fig. 1

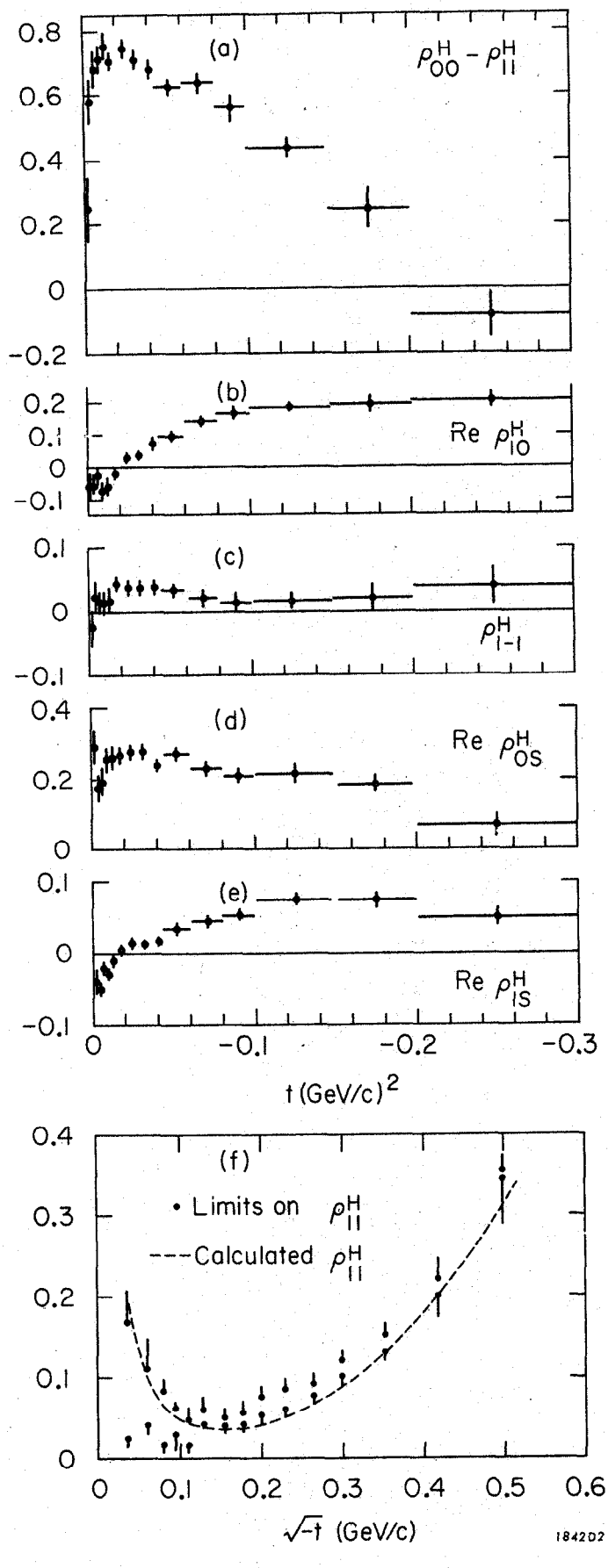
(a)
$\rho^H_{00} - \rho^H_{11}$
(b)
Re ρ^H_{10}
(c)
ρ^H_{1-1}
(d)
Re ρ^H_{0S}
(e)
Re ρ^H_{1S}
t (GeV/c)^2
(f)
• Limits on ρ^H_{11}
---Calculated ρ^H_{11}
$\sqrt{-t}$ (GeV/c)
184202

Fig. 2

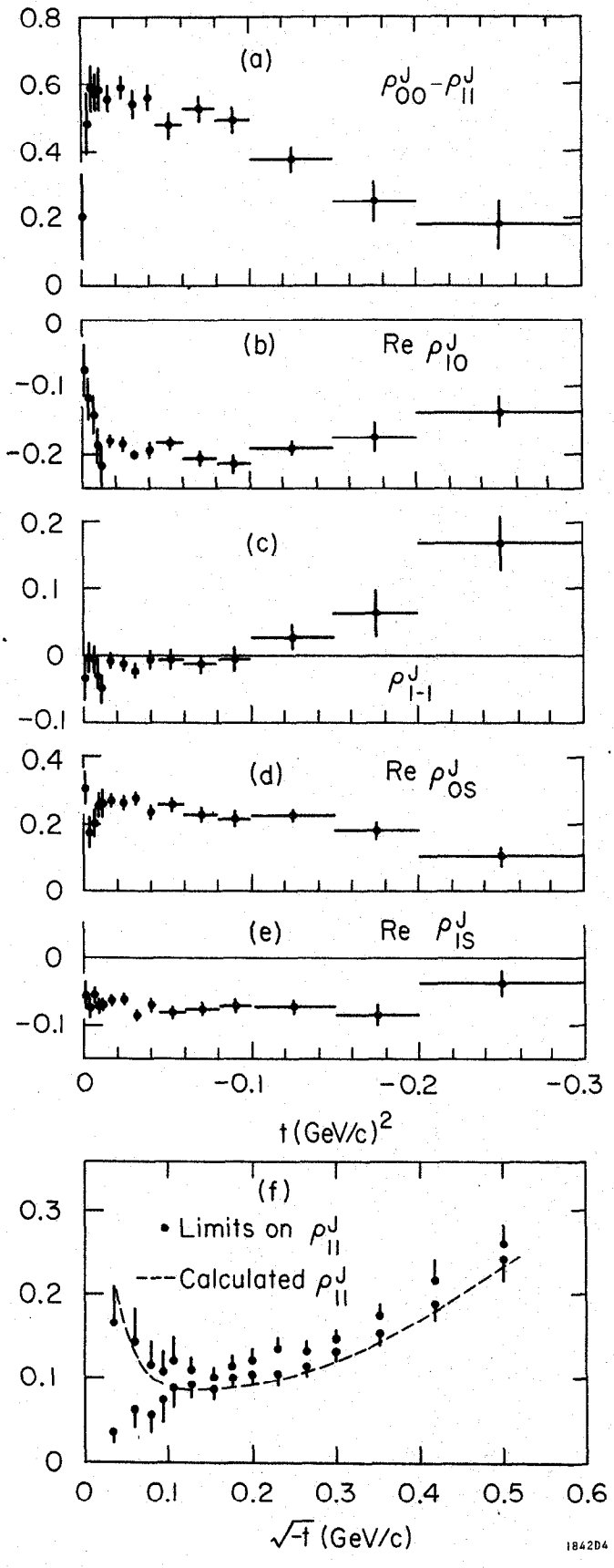
(a)
$\rho^J_{00}-\rho^J_{11}$
(b)
Re ρ^J_{10}
(c)
ρ^J_{1-1}
(d)
Re ρ^J_{0S}
(e)
Re ρ^J_{1S}
$t\,(\mathrm{GeV/c})^2$
(f)
• Limits on ρ^J_{11}
---Calculated ρ^J_{11}
$\sqrt{-t}$ (GeV/c)
1842D4

Fig. 3

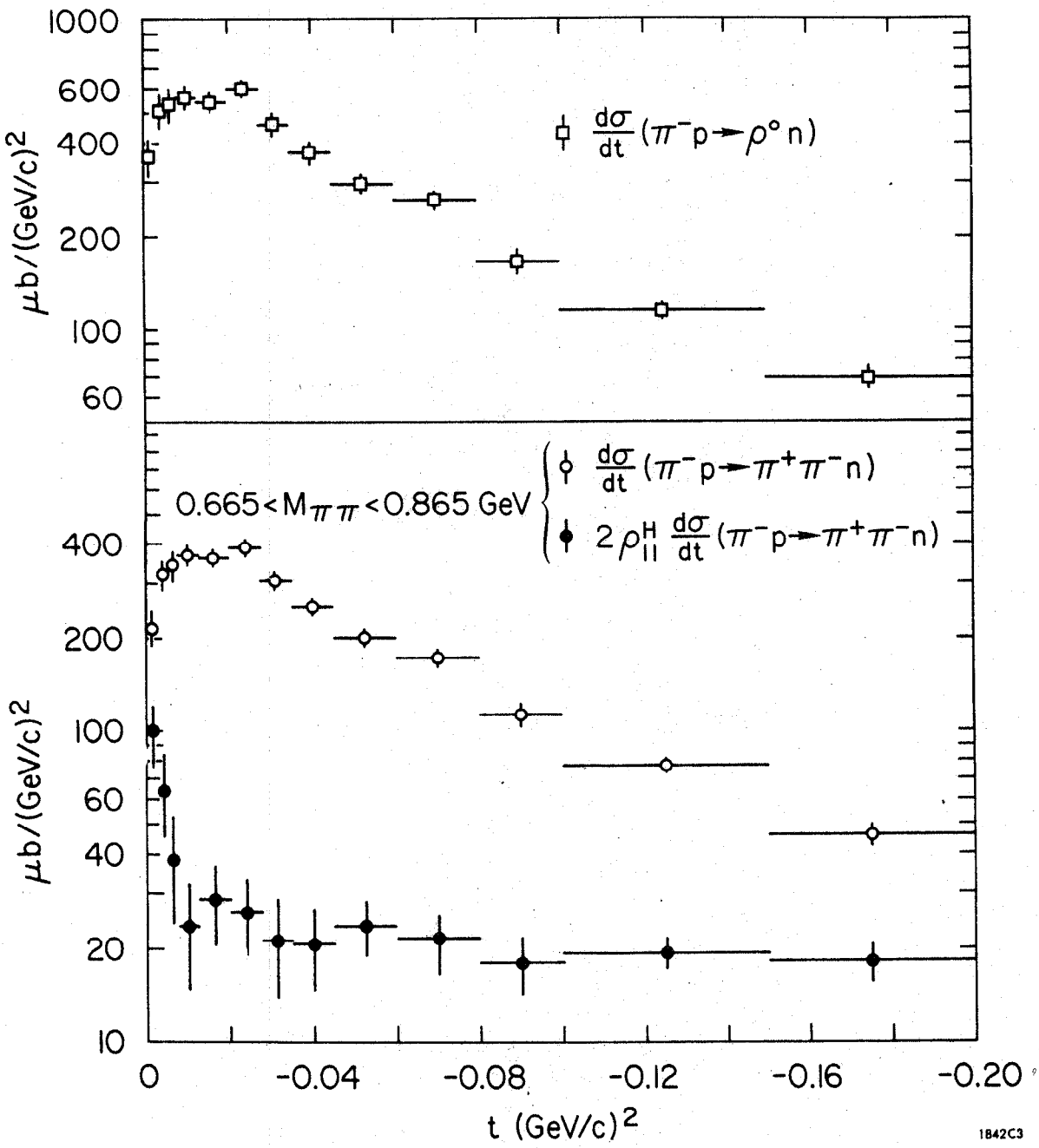
1000
600
400
200
100
60
μb/(GeV/c)²
dσ/dt (π⁻p→ρ°n)
0.665<Mππ<0.865 GeV
dσ/dt (π⁻p→π⁺π⁻n)
2ρ₁₁ᴴ dσ/dt (π⁻p→π⁺π⁻n)
400
200
100
60
40
20
10
μb/(GeV/c)²
0
-0.04
-0.08
-0.12
-0.16
-0.20
t (GeV/c)²
1842C3

Fig. 4

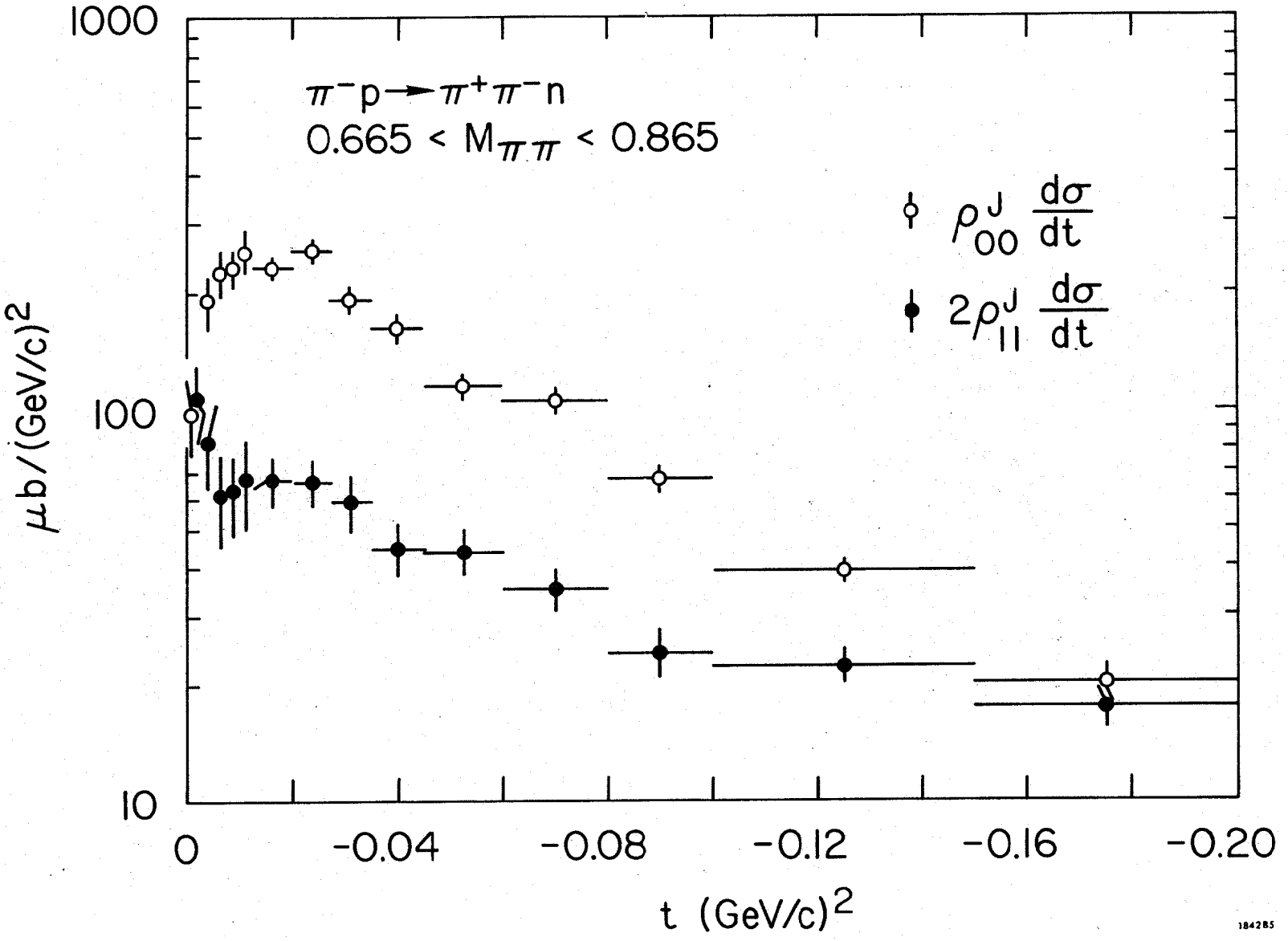
1000
100
10
$\pi^- p \rightarrow \pi^+ \pi^- n$
$0.665 < M_{\pi\pi} < 0.865$
$\rho_{00}^J \frac{d\sigma}{dt}$
$2\rho_{11}^J \frac{d\sigma}{dt}$
$\mu b/(GeV/c)^2$
0
-0.04
-0.08
-0.12
-0.16
-0.20
$t\ (GeV/c)^2$
184285

Fig. 5

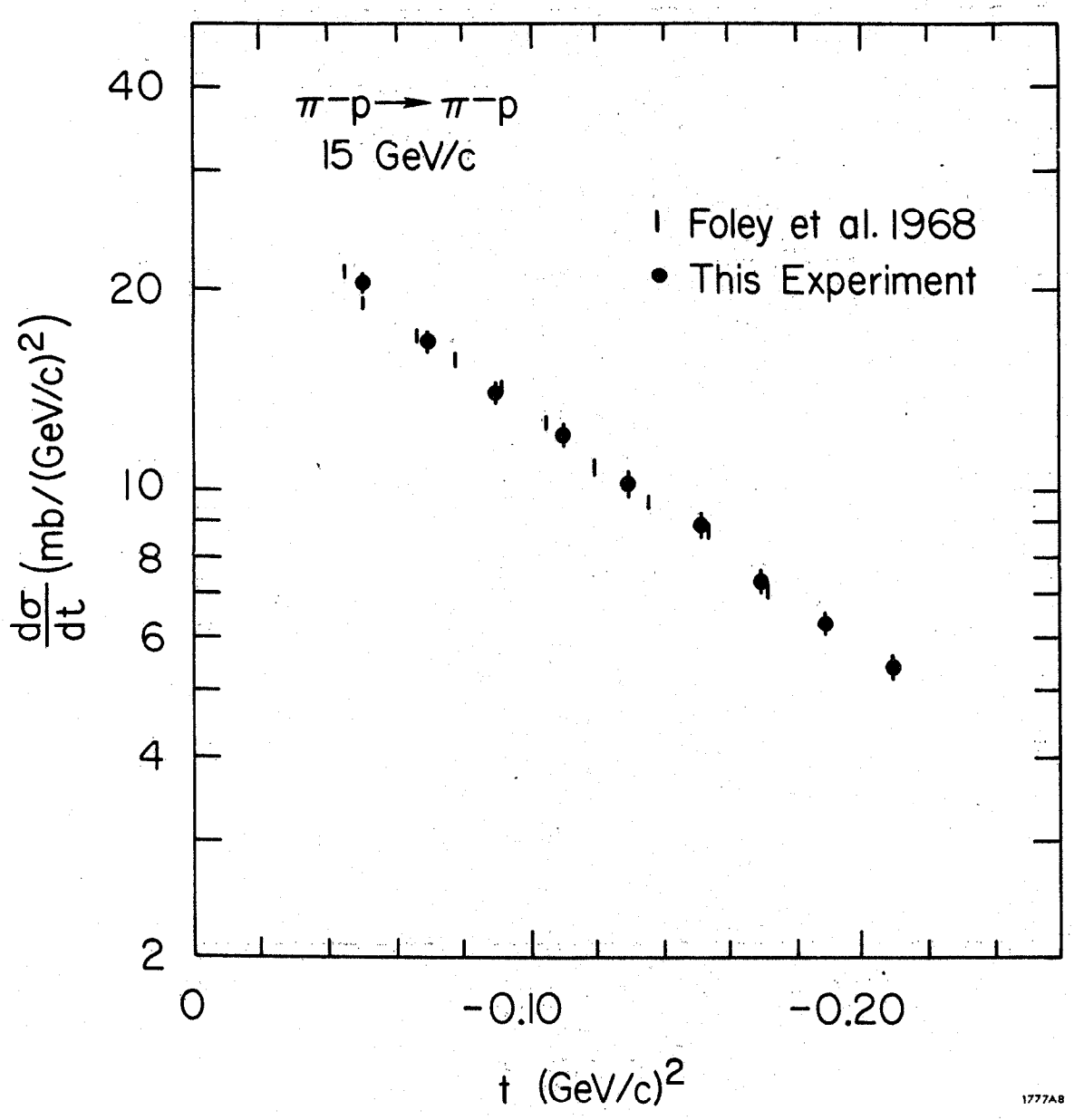
40
20
10
8
6
4
2
0
-0.10
-0.20
$\pi^- p \rightarrow \pi^- p$
15 GeV/c
Foley et al. 1968
This Experiment
$\frac{d\sigma}{dt}$ (mb/(GeV/c)^2)
t (GeV/c)^2
1777A8

Fig. 6

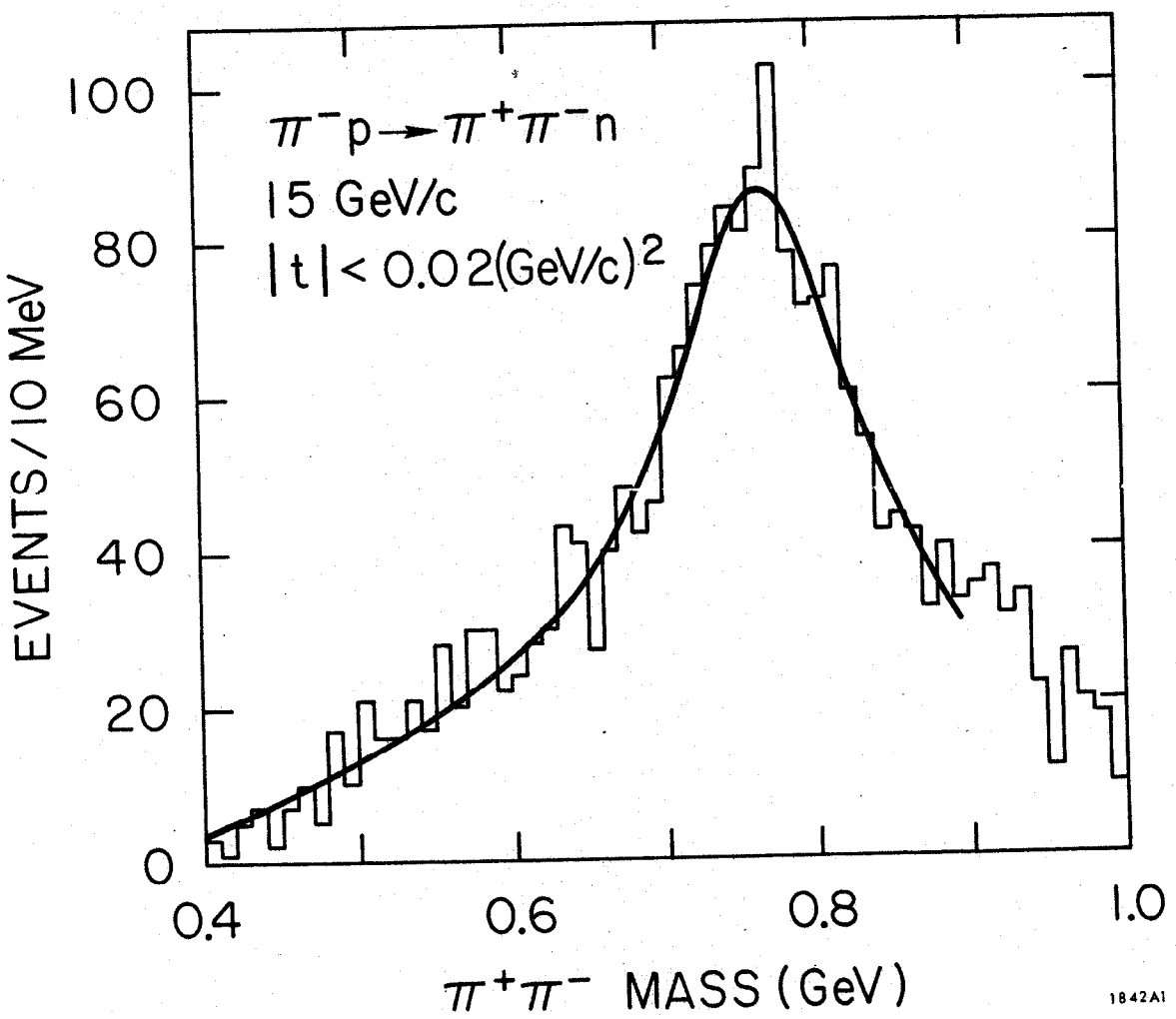
100
80
60
40
20
0
EVENTS/10 MeV
$\pi^- p \rightarrow \pi^+ \pi^- n$
15 GeV/c
$|t| < 0.02 (GeV/c)^2$
0.4
0.6
0.8
1.0
$\pi^+ \pi^-$ MASS (GeV)
1842A1

Fig. 7